
Article:
Johnson, M, Heggs, P and Mahmud, T (2016) Assessment of overall heat transfer coefficient models to predict the performance of laboratory-scale jacketed batch reactors. Organic Process Research & Development, 20 (2). pp. 204-214. ISSN 1083-6160

https://doi.org/10.1021/acs.oprd.5b00378

An assessment of OHTC models to predict the performance of laboratory-scale jacketed batch reactors

Michael Johnson, Peter J. Heggs, and Tariq Mahmud*

Institute of Particle Science and Engineering, School of Chemical and Process Engineering, University of Leeds, Leeds, UK, LS2 9DT

E-mail: t.mahmud@leeds.ac.uk

*To whom correspondence should be addressed

For Table of Contents Only

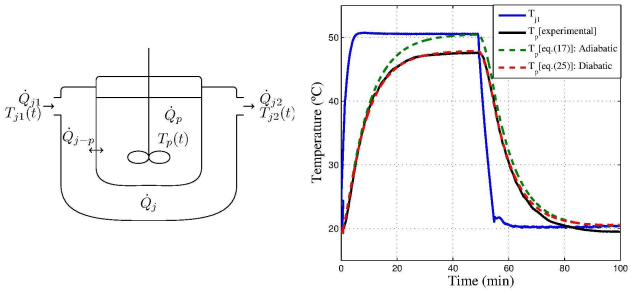

Abstract

Heat transfer models for agitated, jacketed, laboratory-scale batch reactors are required to predict process temperature profiles with great accuracy for tasks associated with chemical process development such as batch crystallisation and chemical reaction kinetics modelling. The standard approach uses a reduced model which assumes the system can be adequately represented by a single overall heat transfer coefficient which is independent of time, however the performance of reduced models for predicting the evolution of process temperature is rarely discussed. Laboratory scale (0.5 and 5 l) experiments were conducted using a Huber thermoregulator to deliver a thermal fluid at constant flow to a heat transfer jacket. It is demonstrated that the relative specific heat contribution of the reactor and inserts represent an increasing obstacle for these transient models with decreasing scale. However, a series of experiments implied that thermal losses were the limiting factor in the performance of a single coefficient reduced model at laboratory-scale. A diabatic model is presented which accounts for both thermal losses and the thermal inertia of the reactor vessel and inserts by incorporating a second coefficient and a modified heat capacity term. The mean absolute error in predicted process temperature was thereby reduced by a factor of eight, from 2.4 to 0.3 K, over a 150 min experiment.

Keywords

heat transfer, OHTC, thermal jacket, thermal effectiveness

Introduction

Jacketed stirred vessels are widely used in the chemical and pharmaceutical industries as well as in the process development laboratories in industry and in academia for carrying out many operations involving heat transfer, for example, chemical reaction and crystallisation processes. Accurate prediction of temperature-time profiles in the vessel as functions of jacket fluid inlet temperature and flow rate is required for controlling these processes to meet product specifications. A *lumped parameter* (or reduced) model with a single overall heat transfer coefficient (OHTC) is frequently employed in industry and academia to predict the transient temperature profiles and batch operating times in such vessels irrespective of the size of the equipment. How adequate and how accurate are the predictions? The OHTC is a steady state concept applied to these transient operations. The reduced model is based on a number of simplifying assumptions as listed in Table 1.[1,2] The use of the OHTC is therefore a compromise between accurately representing the system and the convenience of applying a simple model with only one coefficient. Given this compromise, it is important to provide a measure of OHTC performance in order to clarify how significantly an OHTC-based model departs from real measurements as a consequence of these assumptions.

Some assumptions are more onerous on a model's performance than others, while some assumptions, such as the accommodation of thermal losses and the specific heat contributions of the vessel and inserts can be addressed by using a more involved model. It is therefore possible to redress the compromise between accuracy and simplicity, making it important to select a heat transfer model appropriate for the requirements. A broad estimate of a batch plant's annual throughput and a pharmaceutical/fine chemical batch crystallisation kinetics model are likely to have vastly different requirements for accuracy and complexity. A model which predicts the evolution of process temperature over time to high precision may be more valuable in the latter case.

The OHTC represents the summation of five resistances to heat transfer in series. These are the internal and external film resistances, internal and external fouling resistances (R_{Fi}

Table 1: Assumptions applied in reduced heat transfer models for agitated batch reactors[1,2]

Number	Assumption	Justification
1	The steady state concept of OHTC can be applied to transient operation	Common practice in these models for ease of application
2	The OHTC is constant	Variation of film coefficients with time and position is relatively small
3	Residence time in the jacket is small	When compared to the duration of heating or cooling
4	The process fluid is perfectly mixed	High impeller speed used (large Reynolds number flow)
5	Jacket flow rate is fixed	The thermoregulator has a fixed speed pump
6	Heat capacities are time invariant	Valid when the heat capacities do not depend strongly on temperature and concentration of the reactants
7	The temperature of the jacket inlet is constant	As programmed at the thermoregulator
8	Thermal losses or gains are negligible (the system is adiabatic)	Valid when jacket and process are well insulated
9	Mass weighted heat capacity contributions of the vessel walls, agitator and jacket walls are small in comparison to the process fluid	Frequently true but will depend on the scale, reactants and contruction materials
10	The thermal response of the jacket is instantaneous	Valid when the thermal conductivity is high and the specific heat is low
11	Heat input from the impeller is negligible	When compared to the thermal duty of heating or cooling
12	Heat transfer due to friction in the jacket is negligible	Pressure drop through the jacket is relatively low

and R_{Fo}) and a wall conduction resistance. Depending on the properties of the thermal jacket and process fluids, the fouling resistances are often assumed to be negligible. These resistances are shown as a schematic in Figure 1 and are used to define the OHTC in eq. (1),[3] based on the internal heat transfer area, A_i, of the vessel. It should be noted that the height of the heat transfer area, L, is likely to be affected by vortexing of the process fluid due to agitation as well as by the geometry of the thermal jacket.

$$\frac{1}{U_i A_i} = \frac{1}{\alpha_i A_i} + R_{Fi} + \frac{\ln\left(\frac{D_i}{D_o}\right)}{2\pi L \lambda_w} + R_{Fo} + \frac{1}{\alpha_o A_o} \tag{1}$$

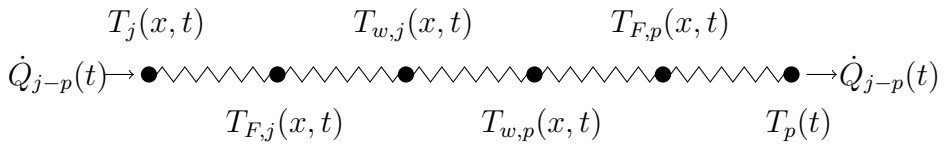

Figure 1: Resistance diagram for heat transfer from the jacket to the process

Countless Nusselt number relationships (expressed in terms of Reynolds and Prandtl numbers) exist for the internal and external film coefficients associated with various vessel geometries, including different impeller types, impeller dimensions, reactor scales and for both Newtonian and non-Newtonian fluids.[4–6] These Nusselt correlations are themselves associated with significant errors, reported as up to 39.8% in Heinlin and Sandal 1972.[7] The dimensionless numbers are calibrated based on instantaneous values of fluid properties, such as dynamic viscosity, which are highly dynamic over a temperature range.

The film coefficients (a_i and a_o) are derived from OHTCs by applying the Wilson method[8] and the 39.8% error does not account for the errors associated with the determination of the OHTC value, which can be significant. Applying these OHTC values reported in the literature to a new system, with even subtle differences in geometry, scale and environmental conditions, can have significant detrimental impact on the capacity to predict the evolution of process temperature with time. Ultimately, relying on literature OHTC values is no substitute to generating a unique OHTC for the precise system at hand, particularly as the model used to obtain the OHTC and the assumptions required for that model are often inadequately reported.

With these factors in mind, there is clear value in providing a quantitative measure for how well a reduced model represents the system. The purpose of the OHTC is to predict

the evolution of process temperature with time. The performance of a heat transfer model can be quantified using the overall mean absolute error (MAE) obtained from the difference between predicted and measured process temperatures over the duration of an experiment. Point temperature data obtained from laboratory-scale batch reactors of 0.5 and 5 l scale are used to assess the performance of OHTC models and investigate the validity of some of the assumptions listed in Table 1.

Experimental Methods

Figure 2 is a schematic of the experimental facility. A Huber 380 HT thermoregulator was connected by flexible hosing to an unbaffled agitated batch reactor (Radleys, UK), of either 0.5 or 5 l scale, mounted in a fume cupboard. The optional condenser, turbidity and pH probes shown in Figure 2 were not used while characterising the heat transfer performance of the system. The vessels have a borosilicate glass construction with a thermal jacket for heat transfer, while the smaller vessel has a secondary jacket providing vacuum insulation to the system. The dished portion of the vessel is not thermally jacketed in the 0.5 l vessel, in contrast to the 5 l vessel. The vessels are agitated by pitched blade impellers. Standard vessel geometry[9] is employed in all aspects except for the impeller to vessel diameter ratios, which are 0.471 and 0.5 for the 0.5 and 5 l scales, respectively, rather than 0.333. The process fluid for this heat transfer study was tap water. Results from the 0.5 l vessel, agitated at 200 rpm are presented as the *base case* in this study.

The Huber delivers a thermal fluid (TF) (Radleys, UK) containing a mixture of triethoxysilanes, to the jacket. The process temperature, T_p, is measured by a class A PTFE Pt100 temperature probe of accuracy within ± 0.15 K at 0 °C. The jacket inlet and outlet temperatures, T_{j1} and T_{j2}, as well as the ambient temperature of the fume cupboard, T_∞, are measured by class B metallic Pt100 temperature probes of accuracy ± 0.3 K at 0 °C. The volumetric flow rate of the TF, delivered by the Huber's fixed speed circulation pump, is

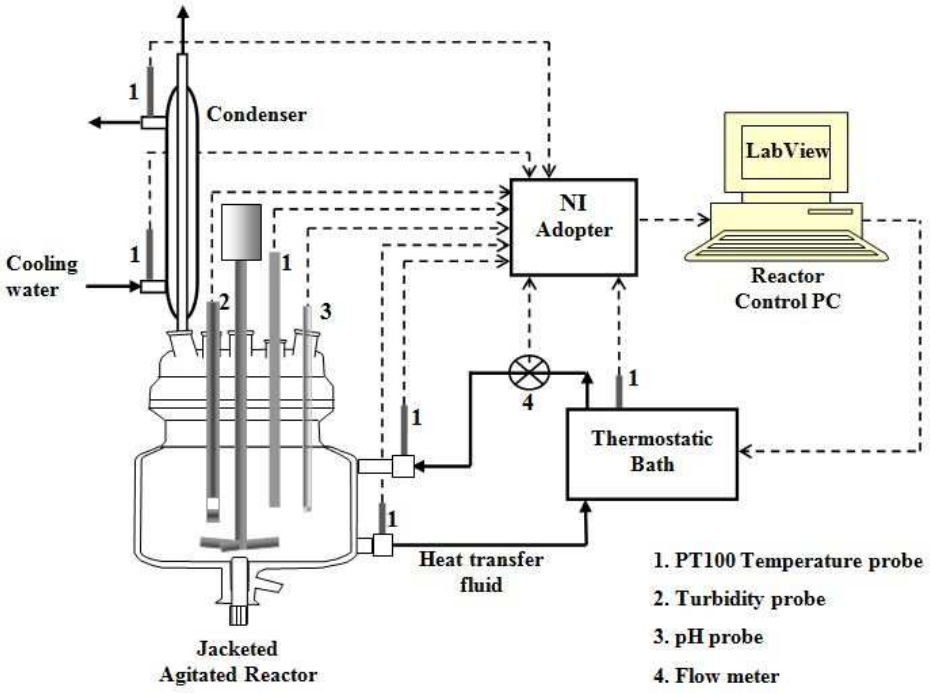

Figure 2: Schematic of the jacketed reactor/crystalliser system with relevant heat transfer and control apparatus

measured to an accuracy of $\pm 1\,\%$ by a positive displacement flow meter (Caché Instrumentation Ltd.). These measurements are recorded at 1 Hz frequency using an in-house, Labview derived data-logging software.

The Huber can be programmed with alternative temperature plans, implemented in Labview, as demonstrated in Figure 3. Temperature plan 1 uses a simple ramp program to cycle the target process temperature, T_{set}, between 20 and 50 °C. Temperature plan 2 uses a near *square step* profile to control the target jacket inlet temperature. Using temperature plan 2, the process temperature is allowed to exponentially approach the jacket temperature, thereby mimicking the natural heating and cooling operation typical of batch crystallisation.

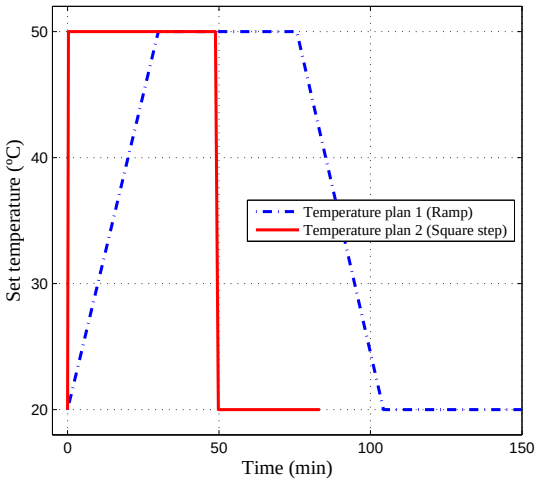

Figure 3: Two set temperature profiles programmed at the Huber thermoregulator

Reduced models for heat transfer

Adiabatic models

The process for heat transfer indicated in Figure 2 is a jacketed batch reactor with a non-isothermal heating/cooling medium flowing through the jacket. Assumption 8, that the system is adiabatic, entails that the entire enthalpy change on the jacket side manifests on the process side, whether the jacket is heating or cooling the process. The heat transfer processes associated with an adiabatic system are illustrated in Figure 4. Consequently, at any instant in time and with assumption 3, the change in enthalpy of the TF flow through the jacket, $\dot{Q}_j(t) = \dot{Q}_{j1}(t) - \dot{Q}_{j2}(t)$, must equal the rate of change of enthalpy in the process, $\dot{Q}_p(t)$, as given by eq. (2). $\dot{Q}_{j-p}(t)$ represents the rate of heat transfer across the wall between the jacket and process and will become relevant later in this derivation.

$$\dot{Q}_j(t) = \dot{Q}_p(t) \tag{2}$$

Measurement of the TF flow, $\dot{M}_j$, and jacket inlet and outlet temperatures enables the calculation of $\dot{Q}_j(t)$, using eq. (3).

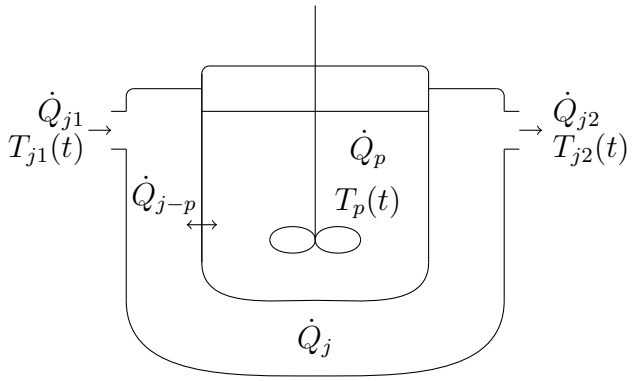

Figure 4: Heat transfer processes in an adiabatic jacketed batch reactor

$$\dot{Q}_j(t) = (\dot{M}c_p)_j(T_{j1}(t) - T_{j2}(t)) \tag{3}$$

The rate of heat accumulation on the process side depends on the application of assumption 9, that the specific heat contributions of the vessel and inserts are negligible compared to the process fluid. If the assumption is applied then $\dot{Q}_p(t)$ is given by eq. (4).

$$\dot{Q}_p(t) = Mc_p\frac{dT_p(t)}{dt} \tag{4}$$

where M is the mass and c_p is the specific heat of the process fluid within the vessel and $T_p(t)$ is the process temperature.

Alternatively, the heat capacity, Mc_p, contributions of all N components of the reactor, including the vessel, agitator and inserts, can influence the process temperature and eq. (4) is updated to give eq. (5).

$$\dot{Q}_p(t) = \sum_{n=1}^{N}(Mc_p)_n\frac{dT_p(t)}{dt} \tag{5}$$

Before proceeding with the reduced model it is useful to check that the assumptions applied are valid for the system under investigation. A common steady state heat exchanger parameter, the thermal effectiveness, E, is proposed for this validation. The thermal effectiveness is the ratio of the actual rate of heat transfer, $\dot{Q}$, to the maximum possible rate of

heat transfer, $\dot{Q}_{max}$, and is represented as follows:

$$E = \frac{\dot{Q}}{\dot{Q}_{max}} \tag{6}$$

The maximum possible rate of heat transfer will occur if the outlet temperature of the TF becomes equal to the process temperature. However, in these batch systems, the temperatures change with time and so the thermal effectiveness will be time dependent. In eq. (6), $\dot{Q}$ will become $\dot{Q}_j(t)$ and $\dot{Q}_{max}$ will be obtained from experimental measurements according to eq. (7):

$$\dot{Q}_{max}(t) = (\dot{M}c_p)_j \left(T_{j1}(t) - T_p(t)\right) \tag{7}$$

Hence the time dependent thermal effectiveness, $E(t)$, can be evaluated from experimental point temperature data using the following ratio of temperatures:

$$E(t) = \left| \frac{(\dot{M}c_p)_j (T_{j1}(t) - T_{j2}(t))}{(\dot{M}c_p)_j (T_{j1}(t) - T_p(t))} \right| = \left| \frac{T_{j1}(t) - T_{j2}(t)}{T_{j1}(t) - T_p(t)} \right| \tag{8}$$

where

$$0 \leq E(t) \leq 1 \tag{9}$$

As a normalised dimensionless parameter, the thermal effectiveness must remain between zero and unity at all times. The failure of this constraint would give cause to question the underlying assumptions of Table 1. Thus, instances where the experimental value for thermal effectiveness is outside the range given by eq. (9) reveal underlying assumptions which undermine the model.

Returning to the reduced model, an OHTC term is required in order to predict the evolution of process temperature with time or predict batch operating times. The OHTC is introduced through the rate of heat transfer across the boundary between the jacket and process, $\dot{Q}_{j-p}(t)$. Since the system is adiabatic, the rate of heat transfer across the boundary

is equivalent to the enthalpy change in the jacket and in the process at any instant.

$$\dot{Q}_j(t) = \dot{Q}_{j-p}(t) = \dot{Q}_p(t) \tag{10}$$

The value ascribed to the OHTC depends on how the temperature difference, representing the driving force for heat transfer, is defined. If the driving force is taken to be the arithmetic mean temperature difference between the jacket and the process temperatures, the OHTC is defined using eq. (11).

$$\dot{Q}_{j-p}(t) = UA(\tilde{T}_j(t) - T_p(t)) \tag{11}$$

where

$$\tilde{T}_j(t) = \frac{T_{j1}(t) + T_{j2}(t)}{2} \tag{12}$$

If the driving force is defined using the more popular logarithmic mean temperature difference, LMTD, eq. (13) applies.

$$\dot{Q}_{j-p}(t) = UA\Delta T_{ln}(t) \tag{13}$$

where

$$\Delta T_{ln}(t) = \frac{\Delta T_1(t) - \Delta T_2(t)}{\ln\left(\frac{\Delta T_1(t)}{\Delta T_2(t)}\right)} = \frac{T_{j1}(t) - T_{j2}(t)}{\ln\left(\frac{T_{j1}(t) - T_p(t)}{T_{j2}(t) - T_p(t)}\right)} \tag{14}$$

As eq. (10) applies at any point in time, eq. (3) and eq. (13) can be equated to provide the relationship for instantaneous jacket outlet temperature in eq. (15).

$$T_{j2}(t) = T_p(t) + (T_{j1}(t) - T_p(t))exp\left(-\frac{UA}{(\dot{M}c_p)_j}\right) \tag{15}$$

Substituting eq. (15) back into eq. (3) and equating that expression with eq. (4) yields the ordinary differential equation (ODE) for process temperature in eq. (16).[10]

$$Mc_p \frac{dT_p(t)}{dt} = (\dot{M}c_p)_j \left(1 - \exp\left(-\frac{UA}{(\dot{M}c_p)_j}\right)\right)(T_{j1}(t) - T_p(t)) \tag{16}$$

Applying eq. (5) rather than eq. (4) to the enthalpy balance results in the modified ODE in eq. (17).

$$\sum_{n=1}^{N} (Mc_p)_n \frac{dT_p(t)}{dt} = (\dot{M}c_p)_j \left(1 - \exp\left(-\frac{UA}{(\dot{M}c_p)_j}\right)\right)(T_{j1}(t) - T_p(t)) \tag{17}$$

The *thermal effectiveness-number of heat transfer units*, $E - NTU$, model proposed by Kays and London 1984[11] introduces alternative terminology for some components of eqs. (16) and (17). The large bracket term represents the thermal effectiveness, previously defined in eq. (6). The grouping in the exponential terms of these equations is labelled the dimensionless number of heat transfer units, NTU, and is the ratio of the heat transfer capacity, UA, of the vessel to the heat capacity of the flow, $\dot{M}c_p$.

$$E = 1 - \exp(-NTU) \tag{18}$$

where

$$NTU = \frac{UA}{(\dot{M}c_p)_j} \tag{19}$$

This highlights a contradiction in the reduced model, because if the thermal effectiveness is a transient term, as implied by eq. (8), the OHTC, which is a steady state concept, must be transient also.

It is possible to solve eq. (16) analytically subject to the conditions in eq. (20). These conditions invoke assumptions 5 and 7, that the TF flow and the jacket inlet temperature are constant. This integration yields eq. (21).[10]

$$\begin{aligned} T_p &= T_p(0) \text{ at} \quad t = 0 \\ T_{j1}, \dot{M} &= \text{constant at} \quad t \geq 0 \end{aligned} \tag{20}$$

$$\ln\left(\frac{T_{j1}-T_p(0)}{T_{j1}-T_p(t)}\right)=\frac{(\dot{M}c_p)_j}{MC_p}\left(1-exp\left(-\frac{UA}{(\dot{M}c_p)_j}\right)\right)t \tag{21}$$

A plot of the logarithmic temperature ratio (LTR) on the left hand side of eq. (21) against time should therefore provide a linear relationship from which the gradient can be used to determine the OHTC. The absence of a straight line relationship indicates the failure of assumption 2 that the OHTC is constant.

Often, the evolution of process temperature must be predicted for a transient jacket inlet temperature. Figure 3 demonstrates two set temperature plans for which the jacket inlet temperature will not be constant during much of the experiment. For a transient jacket inlet temperature, eq. (16) or eq. (17) can be solved numerically subject to the initial conditions in eq. (22).

$$\begin{aligned} T_p &= T_p(0) \text{ at} \quad t=0 \\ \dot{M} &= \text{constant at} \quad t\geq 0 \end{aligned} \tag{22}$$

Here, a second order Runge-Kutta method is used to solve the ODE reduced models in Matlab in order to predict the evolution of process temperature with time for an estimated value of the OHTC. The instantaneous process temperature predicted by any such model, $f(t)$, can be compared with the experimental process temperature measured using the PTFE temperature probe. The OHTC value is optimised by minimising the mean absolute error (MAE) between the predicted and measured process temperature profiles to a tolerance of 1×10^{-4} K. The benefit of this approach is that the optimisation criteria, MAE, is calculated over the entire duration of the experiment, rather than for a brief period when the jacket inlet temperature is held constant.

$$\text{MAE}=\frac{1}{\text{I}}\sum_{i=1}^{\text{I}}|f(t)-T_p(t)|_i \tag{23}$$

This MAE provides a quantitative measure of the performance of the model and can be

used as a basis for comparing the different ODE models. By comparing the predicted and measured process temperature profiles it is also possible to identify the regions where the profiles depart and thereby deduce which assumptions most limit the model's performance.

Diabatic model

A poorly insulated, laboratory-scale glass batch reactor, with a corresponding large external surface area to volume ratio, is unlikely to have negligible thermal losses. For a diabatic system, as demonstrated in Figure 5, eqs. (3), (4) and (13) cannot be equated due to thermal losses both direct from the process through the reactor lid and from the jacket external wall. The schematics in Figures 4 and 5 are largely representative of the larger 5 l reactor used in this study as the thermal jacket covers the dished portion of the process and there is no secondary vacuum jacket to reduce thermal losses.

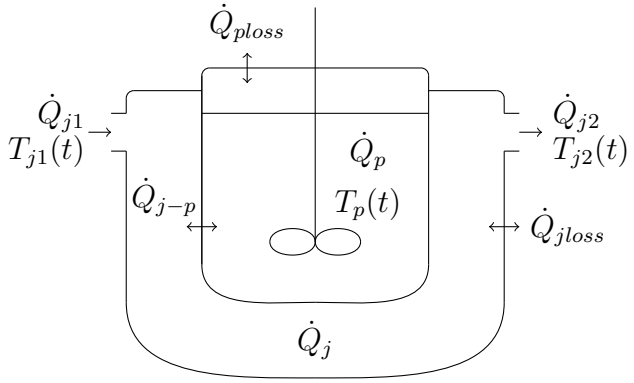

Figure 5: Heat transfer processes in a diabatic jacketed batch reactor

A heat balance around the process side reveals that the sum of the rate of heat accumulation in the process, $\dot{Q}_p(t)$, and the rate of heat loss from the process, $\dot{Q}_{ploss}(t)$, is equal to the rate of heat transfer across the wall between the jacket and the process, $\dot{Q}_{j-p}(t)$. Equally, a heat balance around the jacket indicates that the difference between the total rate of heat transfer from the jacket, $\dot{Q}_j(t)$, and the rate of heat loss from the jacket, $\dot{Q}_{jloss}(t)$, equates to the rate of heat transfer across the boundary, $\dot{Q}_{j-p}(t)$.

$$\dot{Q}_p(t) + \dot{Q}_{ploss}(t) = \dot{Q}_{j-p}(t) = \dot{Q}_j(t) - \dot{Q}_{jloss}(t) \tag{24}$$

The rate of thermal loss from the process is introduced to eq. (17), generating eq. (25). In reality, these thermal losses represent the sum of the losses due to radiation and free convection, however for simplicity the rate of heat loss is represented using a single coefficient, similar to eq. (11) for heat transferred across the interior jacket wall. This *lumped parameter* thermal loss model used implies that the vapour in the vessel ullage is in thermal equilibrium with the process fluid. The driving force for heat loss from the process is given by the difference between the process temperature and the ambient temperature, $T_\infty(t)$.

$$\sum_{n=1}^{N} (Mc_p)_n \frac{dT_p(t)}{dt} = (\dot{M}c_p)_j \left(1 - exp\left(-\frac{UA}{(\dot{M}c_p)_j}\right)\right)(T_{j1}(t) - T_p(t)) - (UA)_{ploss}(T_p(t) - T_\infty(t)) \tag{25}$$

This diabatic ODE model given by eq. (25) can be integrated using the same second order Runge-Kutta numerical integration technique.[12] However, the ODE must now be optimised for two heat transfer coefficients, U and U_{ploss}, thus requiring more extensive experimental validation.

Since the rate of heat transfer across the interior jacket wall and rate of heat transfer from the jacket are known at any instant in time, the rate of thermal loss from the jacket external wall can be determined from eq. (24). The heat transfer coefficient for the losses from the jacket can be determined without the need for numerical integration using eq. (26).

$$(\dot{M}c_p)_j(T_{j1}(t) - T_{j2}(t)) - (UA)_{jloss}(\tilde{T}_j(t) - T_\infty(t)) = (\dot{M}c_p)_j \left(1 - exp\left(-\frac{UA}{(\dot{M}c_p)_j}\right)\right)(T_{j1}(t) - T_p(t)) \tag{26}$$

Results

Measured temperature profiles

Measured temperature-time profiles for the base case heating-cooling run in the 0.5 l vessel are shown in Figure 6 for the ramp and natural heating/cooling operations of temperature plans 1 and 2. The process fluid is agitated at an impeller speed of 200 rpm with corresponding Re ($\frac{\rho N {D_i}^2}{\mu}$) $\approx$ 47000. The jacket outlet temperature is also measured but closely mirrors the inlet temperature, due to the rapid flow of the TF in the jacket, and hence is not shown.

From the response of the process temperature to the jacket temperature profiles, it is possible to observe departure from some of the assumptions listed in Table 1. At the onset of heating at the start of Figure 6a and at the onset of cooling in Figure 6b at 50 min there is a clear delay in the response of process temperature to the rapid change in temperature on the jacket side. This demonstrates the thermal inertia of the glass vessel in contradiction of assumption 9 that the heat capacity contribution of the vessel is negligible in comparison to the process fluid.

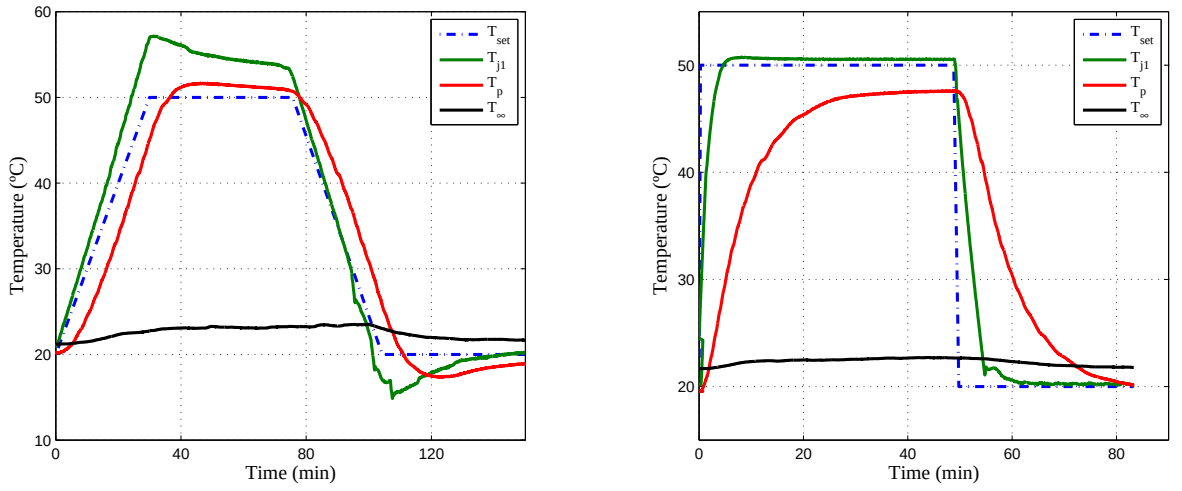

(a) Temperature plan 1 (ramp operation)

(b) Temperature plan 2 (natural heating/cooling operation)

Figure 6: Measured temperature-time profiles in the 0.5 l reactor agitated at 200 rpm

Figure 6b demonstrates the process temperature approaching steady state between 30

and 50 min, peaking at a maximum of 47.6 °C, significantly below that of the jacket inlet temperature of 50.5 °C. Similarly in Figure 6a, between 45 and 80 min, the process temperature falls in spite of the higher jacket inlet temperature and hence the positive driving force for heat transfer between the jacket and process. This demonstrates the diabatic nature of the system as a result of heat loss directly from the process in contravention of assumption 8. In an adiabiatic system, the process temperature would approach the jacket temperature and the temperature drop through the jacket would fall towards zero. Here, the maximum process temperature is limited by the thermal losses while a near constant temperature drop is maintained on the jacket side.

Between 5 and 50 min in Figure 6b both the jacket inlet temperature and the ambient temperature are relatively constant. Consequently, as the process temperature rapidly increases towards the jacket temperature the driving force for desirable heat transfer to the process quickly falls, while the driving force for undesirable thermal losses from the process increases. The assumption that thermal losses are negligible is therefore most applicable at the start of the heating regime, however, as the thermal losses are greatest in magnitude when heat transfer to the process is at a minimum, thermal losses can have a significant influence on the process temperature profile towards the end of the heating regime.

Having identified a couple of assumptions which appear to be qualitatively contradicted by the raw temperature data, we can quantitatively assess how these assumptions affect the capacity of the models proposed to predict the evolution in process temperature over time.

Transience of the OHTC

As listed in Table 1, the OHTC is assumed to be constant with time in reduced models. Two methods are outlined for testing this assumption using eqs. (18) and (21). Figure 7 demonstrates the evolution in thermal effectiveness over the duration of temperature plan 1, as calculated from eq. (8), for the base case experiment. From this thermal effectiveness profile, an instantaneous OHTC is calculated using eqs. (18) and (19). If the thermal re-

sponse of the jacket is not instantaneous and the system is diabatic, achieve negative thermal effectiveness values may be obtained from the experimental data, therefore the modulus of the thermal effectiveness is shown in Figure 7 for representation on a logarithmic scale.

An OHTC of 208.9 $\mathrm{W\,m^{-2}\,K^{-1}}$ was found by optimising eq. (17) for the minimum MAE over the entire duration of the experiment and is shown for reference in Figure 7. Typical OHTC values reported in the literature for glass lined stainless steel reactors lie in the range of 170-450 $\mathrm{W\,m^{-2}\,K^{-1}}$.[13]

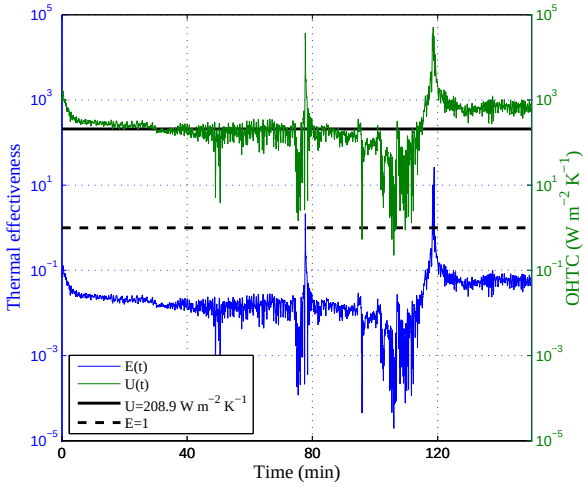

Figure 7: Evolution of thermal effectiveness (blue) and the OHTC (green) with time, obtained from eqs. (8) and (18) respectively, during temperature plan 1

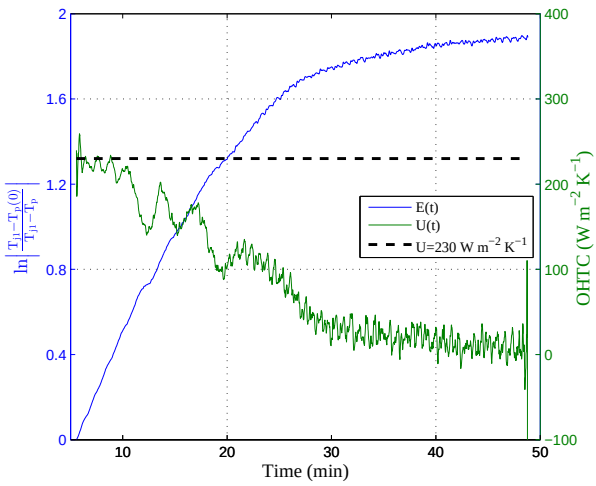

Figure 8: Evolution of the logarithmic temperature ratio (LTR) (blue) and OHTC (green) with time, obtained from eqs. (21) and (27) respectively, during the 5-50 min period of temperature plan 2 (where T_{j1} = constant)

The asymptotes at around 80 and 115 min coincide with the thermal effectiveness exceeding unity. This contravenes the constraint shown in eq. (9) and thus implies a failure in the assumptions of Table 1 at these times. Comparing, this thermal effectiveness profile with the corresponding raw temperature data in Figure 6a, the thermal effectiveness asymptotes coincide with the jacket and process temperatures becoming equal during a transition between heating and cooling operation.

If there is a transition between heating and cooling, there must be an instant where

there is no driving force for heat transfer between the jacket and process. Logic follows that if there is no temperature difference between the jacket and process there can be no heat transfer between the jacket and process and the thermal effectiveness must be zero. However, as the thermal response of the jacket to rapid changes in jacket inlet temperature is not instantaneous and the jacket is imperfectly insulated, in contradiction of assumptions 10 and 8 respectively, a finite temperature drop is maintained along the length of the jacket while there is no driving force for heat transfer to the process. Consequently, during rapid changes in jacket inlet temperature and when the process temperature approaches the jacket inlet temperature, maximum strain is placed on the adiabatic reduced heat transfer model and the thermal effectiveness tends to infinity.

In Figure 6b the jacket inlet temperature is near constant between 5 and 50 minutes, thereby satisfying the conditions in eq. (20) which allow eq. (16) to be solved analytically, generating eq. (21). Figure 8 shows a plot of the LTR term (left hand side of eq. (21)) evolving with time. A constant gradient in this relationship would imply a constant OHTC. The instantaneous OHTC obtained from eq. (26) using the instantaneous gradients of the LTR-time curve is also plotted on a second axis of Figure 8. The instantaneous LTR-time gradients are time averaged over two minute intervals in order to reduce the noise arising from fluctuations in the experimental measurements.

$$U(t)A = -(\dot{M}c_p)_j \ln\left(1 - \frac{(\dot{M}c_p)_j}{MC_p}\left(\frac{d\ln\left(\frac{T_{j1}(t)-T_p(0)}{T_{j1}(t)-T_p(t)}\right)}{dt}\right)\right) \tag{27}$$

In Figure 8 the LTR profile has a near constant gradient during 5-12 min, falls significantly during 12-30 min and is very small thereafter. Consequently, even while the jacket inlet temperature and jacket flow rate are constant, there are difficulties in generating a clear and unambiguous constant OHTC from the experimental data. During the initial 5-12 min time range, the instantaneous OHTC is close to the value of $208.9\,\mathrm{W\,m^{-2}\,K^{-1}}$ generated using eq. (17). During this period the driving force for heat transfer to the process is high and

that for thermal loss from the process is very low and so the assumption that thermal losses are negligible is most applicable in this regime. As the process temperature rises, the thermal losses become increasingly significant and, as the thermal losses approach equilibrium with the desirable heat transfer to the process, there is negligible heat accumulation in the process the observed OHTC falls toward zero.

Specific heat contributions of the vessel and inserts

During a heating cycle, the TF heats not only the process fluid, but the metal and glass walls of the vessel and all inserts on the process side, which could include impellers and baffles for mixing, as well as temperature and other measurement probes. As a result of assumption 9, only the heat capacity of the process fluid is considered in eq. (16), implying that the wall separating the jacket and process is transparent to heat, even though the OHTC itself contains a wall conduction term, as shown in eq. (1).

Table 2 details the heat capacity contributions of the various components of four water filled, unbaffled reactors of different scales, including the two laboratory-scale reactors investigated in this study. For this exercise, heat transfer is assumed to be in one direction, either from the jacket to the process or vice versa, and so only the reactor wall separating the jacket and process is considered to contribute towards the heat capacity of the vessel. The majority of the total heat capacity is accounted for by the process fluid, however the contribution of the vessel and inserts are by no means negligible. The heat capacity contributions of the vessel and inserts increases as scale is reduced as a consequence of the enhanced surface area to volume ratio. The vessel and inserts represent 20.8 and 17.6 % of the total heat capacities of the filled 0.5 and 5 l reactors respectively.

When the vessel and inserts contribute appreciably to the total system heat capacity, the heat capacity term in eq. (16) is smaller than that in eq. (17). When using a particular model to optimise the OHTC to the experimental data, the specific heat, thermal effectiveness, number of heat transfer units and OHTC are all proportional, and so eq. (16) will estimate a

Table 2: Contributions to the total specific heat of water filled, agitated batch reactors of different scales

	V (m^3)	M (kg)	c_p ($kJ\,kg^{-1}\,K^{-1}$)	Mc_p ($kJ\,K^{-1}$)	Mc_p (%)
2273 litre (Pfaudler, USA)[14]					
Water	2.27	2.26×10^3	4.18	9.45×10^3	96.2
Steel inserts	2.37×10^{-3}	1.87×10^1	0.51	9.54	0.1
Steel walls	8.96×10^{-2}	7.07×10^2	0.51	3.60×10^2	3.7
Total				9.82×10^3	
25 litre (Radleys, UK)					
Water	2.15×10^{-2}	2.14×10^1	4.18	8.93×10^1	94.8
Teflon inserts	2.23×10^{-4}	4.80×10^{-1}	1.30	6.24×10^{-1}	0.7
Glass walls	2.53×10^{-3}	5.65	0.75	4.23	4.5
Total				9.42×10^1	
5 litre (Radleys, UK)					
Water	4.31×10^{-3}	4.28	4.18	1.79×10^1	82.4
Teflon inserts	2.10×10^{-5}	4.60×10^{-2}	1.30	5.98×10^{-2}	0.3
Glass walls	7.60×10^{-4}	5.02	0.75	3.77	17.3
Total				2.17×10^1	
0.5 litre (Radleys, UK)					
Water	4.29×10^{-4}	4.26×10^{-1}	4.18	1.78	79.2
Teflon inserts	2.00×10^{-5}	4.30×10^{-2}	1.30	5.59×10^{-2}	2.5
Glass walls	1.00×10^{-4}	5.49×10^{-1}	0.75	4.12×10^{-1}	18.3
Total				2.25	

lower thermal effectiveness and OHTC than eq. (17) for the same experimental data. Table 3 demonstrates that the OHTC value found using eq. (17) is 13.3 % higher than that obtained using eq. (16) for the 0.5 l vessel and 22 % higher for the 5 l vessel. It is therefore vital, particularly at laboratory-scale, to understand how the heat capacity of the system has been estimated for the purpose of calculating the OHTC, and yet this is not always explicit when OHTC values are reported in the literature.

Table 3 confirms that the two models perform equally well in predicting the evolution of process temperature when the same specific heat assumption is used in the generation and application of the OHTC. The significance of the heat capacity assumption becomes clear in Figure 9 when different heat capacity models are used to optimise the OHTC and apply the OHTC to predict the evolution of process temperature. The dashed lines of Figure 9

Table 3: The impact of the specific heat contributions of the vessel and inserts towards the OHTC for 0.5 l and 5 l vessels

Scale (l)	Model	Mc_p ($kJ\,K^{-1}$)	UA ($W\,K^{-1}$)	U ($W\,m^{-2}\,K^{-1}$)	MAE (K)	Max error (K)
0.5	eq. (16)	1.78	3.59	184.4	2.36	3.39
0.5	eq. (17)	2.25	4.07	208.9	2.36	3.39
5	eq. (16)	1.79×10^1	9.92	83.4	1.20	2.10
5	eq. (17)	2.17×10^1	12.10	101.8	1.20	2.10

represent model predictions of process temperature. The first legend entry for these profiles represents the model used to estimate the OHTC and the second legend entry represents the model used to predict the temperature profile.

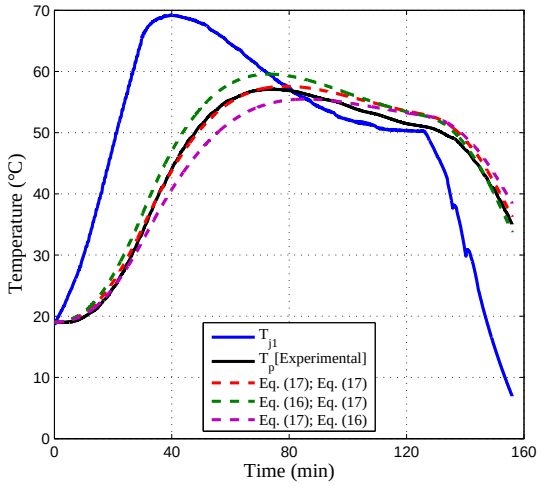

Figure 9: The effect of heat capacity assumptions on the predicted process temperature profile in a 5 l reactor agitated at 200 rpm. Dashed lines represent predictions of process temperature where either eq. (16) or eq. (17) has been used to optimise the OHTC (first legend entry) before predicting the evolution of process temperature (second legend entry)

If the low OHTC, optimised using eq. (16), is applied in eq. (17) the thermal effectiveness will be artificially low for the heat capacity term. When predicting the evolution process temperature, eq. (17) will correct for the low thermal effectiveness by over-estimating the rate of change in process temperature. The predicted process temperature therefore over-shoots the experimental process temperature, as shown by the green line of Figure 9. Conversely, if the larger OHTC, optimised using eq. (17), is deployed in eq. (16) the heat capacity is too

low for the thermal effectiveness and the predicted process temperature profile will undershoot the experimental data, as shown by the purple line of Figure 9. This highlights the risk associated with indiscriminately applying OHTCs from the literature without appreciating the full calculation procedure.

Thermal losses from and gains by the system

An adiabatic model with just one coefficient in eq. (17) and a diabatic model with two coefficients in eq. (25) are presented to predict the evolution of process temperature with time. The experimental temperature profiles in Figure 6 imply that thermal losses from the process are not negligible. However, the approach used for numerical intergation of ODEs throughout this study provides a quantitative measure of how well each heat transfer model performs in predicting process temperature over time and so the significance of thermal losses can be assessed.

Using this methodology, an OHTC is optimised by solving the ODE for the minimum MAE over the duration of any particular experiment. The second heat transfer coefficient governing thermal loss from the process is assumed to be constant for each vessel. This coefficient can therefore be optimised across multiple experiments undertaken in a particular vessel, including for experiments using different jacket inlet temperature profiles and different mixing conditions.

The optimised coefficients from each model are presented for the two temperature plans, using the base case experimental set up, in Table 4. The MAE and maximum error in the predicted process temperature are also presented as a measure of each model's performance. The process temperature predictions of each model can also be qualitatively compared with the measured process temperature profiles in Figure 10.

In Figure 10, the adiabatic model is shown to significantly over-predict the process temperature whenever the process temperature is significantly larger than the ambient temperature and hence the driving force for thermal loss is high. Consequently errors up to 3.4

Table 4: A summary of OHTCs and performance of adiabatic (eq. (17)) and diabatic (eq. (25)) heat transfer models in the 0.5 l vessel agitated at 200 rpm

Temperature plan	Model	UA ($W K^{-1}$)	U ($W m^{-2} K^{-1}$)	$(UA)_{ploss}$ ($W K^{-1}$)	MAE (K)	Max error (K)
Plan 1	eq. (17)	4.07	208.9	-	2.4	3.4
Plan 1	eq. (25)	4.25	218.0	0.45	0.3	0.8
Plan 2	eq. (17)	4.49	230.3	-	1.7	2.9
Plan 2	eq. (25)	4.25	218.0	0.45	0.5	1.1

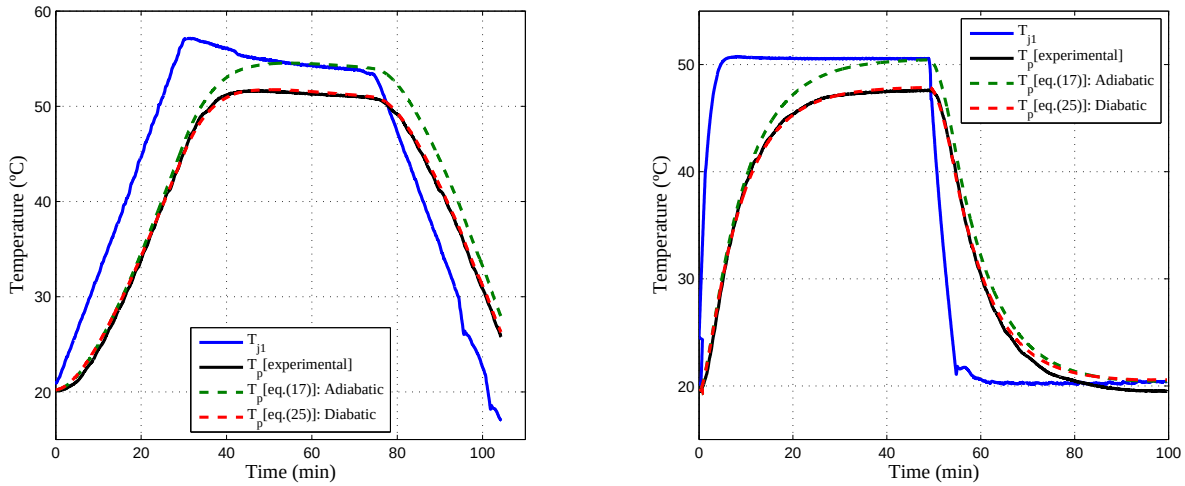

(a) Temperature plan 1

(b) Temperature plan 2

Figure 10: A comparison of adiabatic (eq. (17)) and diabatic (eq. (25)) ODE models for predicting the evolution of process temperature with time in a 0.5 l vessel agitated at 200 rpm

and 2.9 K are observed in each temperature plan and the MAE associated with temperature plan 1 is 2.4 K. This MAE is a factor of eight lower when applying the diabatic model to temperature plan 1, equivalent to the experimental error associated with the class B temperature probes used to measure the jacket inlet and outlet temperatures and the ambient temperature. Figure 10 also demonstrates the exceptionally close fit between the diabatic model predictions for process temperature and the experimental data throughout the two experiments.

Significantly, the optimum OHTC generated by the adiabatic model is 10.3 % larger for temperature plan 2 than for temperature plan 1, even though all the experimental conditions

apart from the jacket inlet profile are identical. The maximum jacket inlet temperature and maximum process temperature are both larger for temperature plan 1 and so the thermal losses impact that experiment more significantly. Consequently, thermal losses not only significantly limit the quality of the predictions of the adiabatic model, but the applicability of the OHTC generated is also more limited as the thermal losses impact experiments with different jacket inlet profiles differently. Conversely, the adiabatic model performs very well using the same two heat transfer coefficients for the two different jacket inlet temperature profiles. Therefore, even though eq. (25) must be optimised for a second coefficient in addition to the OHTC, a greater number of unique coefficients may be required if the adiabatic eq. (17) model is applied to multiple experiments with different jacket inlet temperature profiles.

Summary of the procedure for characterising heat transfer in jacketed batch vessels

The following procedure is recommended for characterising heat transfer in jacketed batch reactors prior to undertaking chemical reactions or crystallisations in that vessel:

- A target, or set point, process temperature profile should be chosen in consideration of the crystallisation or reaction experiments to be undertaken in the vessel. Two alternative temperature profiles are shown in Figure 3.
- A minimum of four temperature probes and one in-line flow meter are required at the locations indicated in Figure 2 in order to capture the five fundamental parameters necessary to characterise the system. These parameters are T_{j1}, T_{j2}, T_p, T_∞, and $\dot{M}$.
- Simple experiments should be conducted using the chosen set point temperature profile on the process side and a chemically inert process fluid, recording the transient temperatures and jacket flow at short regular intervals.

- Data should be analysed in order to characterise the system and to find a heat transfer model which adequately represents the system. The thermal effectiveness, $E(t)$, may be calculated as a function of time using Equation (8). If $E(t)$ exceeds unity at any point in time, this indicates the failure of an assumption listed in Table 1 at these stages of the experiment.

- A heat transfer model must be chosen to predict the evolution of process temperature with time. Two adiabatic models are presented using different assumptions regarding the thermal inertia of the vessel and inserts in eqs. (16) and (17), and a diabatic model is presented in eq. (25). The system in this study is best represented by eq. (25), however, the heat transfer model should be chosen based on the the limiting assumptions for the relevant system, revealed from the $E(t)$ profile.

- The lumped model parameter, UA, must be optimised using the chosen heat transfer model and an assessment made regarding how well that model performs when predicting process temperature evolving with time. Numerical integration of the ODE for an estimate of UA enables the calculation of an error such as the MAE given in eq. (23). The OHTC is optimised by manipulating UA to find its value when the MAE is at a minimum. The MAE and the maximum departure between the experimental and predicted process temperatures provide measures of the performance of the chosen model using the optimised OHTC. An informed judgement can then be made as to whether these errors are acceptably low for the work to be undertaken or whether an alternative model is required.

Conclusions

1. Heat transfer in agitated, jacketed batch reactors is a transient process, however heat transfer to the process is typically predicted using reduced models which employ a single OHTC which is independent of time. Depending on how the reduced model

assumptions are employed, vastly different OHTC values can be determined from the same experimental data. For a 0.5 l vessel agitated at 200 rpm, modifying these assumptions resulted in the OHTC varying in the range of 184.4-230.3 $\mathrm{W\,m^{-2}\,K^{-1}}$, a variation of 20 %.

2. The evolution in thermal effectiveness over time provides a useful check as to whether these assumptions adequately represent the system at any instant in time. Solving ODEs of reduced heat transfer models numerically allows a solution to be found for a transient temperature profile in the jacket. This approach also provides a quantitative measure of the reduced model's performance in predicting process temperature evolving over time through the MAE and the maximum error.

3. The specific heat contribution of the vessel and inserts become increasingly significant at laboratory-scale as vessel walls and inserts increasingly contribute towards the total mass of the system with reduced capacity. Whether these specific heat contributions have been considered in the estimation of the OHTC can have a significant impact on the value of the OHTC and the quality of any predictions attained using this value.

4. The large surface area to volume ratio and imperfect insulation of glass walled, laboratory-scale batch reactors challenges the underlying assumption that the system is adiabatic. Incorporating even a simple thermal loss model to the ODE has been observed to reduce the MAE by a factor of up to eight, while the model also becomes more robust in its application to different jacket inlet temperature profiles.

5. For the laboratory-scale jacketed batch reactors in this study, a diabatic reduced model which incorporates the heat capacity of the vessel and inserts, presented in eq. (25), best represents the heat transfer and can be used to predict the evolution of process temperature to a high precision. In order to reach this conclusion the equipment needed to be characterised by measuring jacket inlet and outlet, process and ambient temperatures as well as the jacket flow rate during a series of simple experiments. It is

essential to consider and then assess the most appropriate heat transfer model before proceeding to an investigation of crystallisation, mixing or reaction kinetics for process development.

Nomenclature

α Heat transfer film coefficient ($\mathrm{W\,m^{-2}\,K^{-1}}$)

$\dot{M}$ Mass flow ($\mathrm{kg\,s^{-1}}$)

$\dot{Q}$ Rate of heat transfer (W)

A Heat transfer area ($\mathrm{m^2}$)

c_p Specific heat capacity ($\mathrm{W\,kg^{-1}\,K^{-1}}$)

D Diameter (m)

E Thermal effectiveness

L Height of heat transfer area ($\mathrm{W\,m^{-1}\,K^{-1}}$)

M Mass (kg)

MAE Mean absolute error (K)

NTU Number of heat transfer units

$OHTC$ Overall heat transfer coefficient ($\mathrm{W\,m^{-2}\,K^{-1}}$)

R Resistance to heat transfer ($\mathrm{W\,K^{-1}}$)

T Temperature (K)

t Time (s)

U Heat transfer coefficient ($\mathrm{W\,m^{-2}\,K^{-1}}$)

x Length along jacket wall (m)

λ Thermal conductivity (m)

Subscripts

1 inlet

2 outlet

F fouling

i interior

j jacket

$j-p$ jacket to process

max maximum

o exterior

p process

w wall

Acknowledgements

Thank you to Neil Smith for his assistance in the laboratory and to Steve Terry for his experise in programming the Labview software for data-logging and reactor temperature control used in this study. Thanks also to Radleys UK for their support in the operation and maintenance of the Huber.

References

(1) Baker, C. K.; Walter, G. H. *Heat Transfer Engineering* **1979**, *1*, 28–40.

(2) Heggs, P. J.; Hills, P. D. *Heat Exchange Engineering Vol. 4*; Honeysuckle International Publications, 1994; Vol. 4; Chapter 14.

(3) Fernandez-Seara, J.; Uhía, F. J.; Sieres, J.; Campo, A. *Applied Thermal Engineering* **2007**, *27*, 2745–2757.

(4) Bondy, F.; Lippa, S. *Chemical Engineering (New York)* **1983**, *90*, 62–71.

(5) Chapman, F. S.; Holland, F. A. *Chemical Engineering (New York)* **1965**, *18*, 153–158.

(6) Mohan, P.; Nicholas Emery, A.; Al-Hassan, T. *Experimental Thermal and Fluid Science* **1992**, *5*, 861–883.

(7) Heinlin, H. W.; Sandal, O. C. *Ind. Eng. Chem. Process Des. Develop.* **1972**, *11*, 490–495.

(8) Wilson, E. E. *Trans. Am. Soc. Mech. Engrs.* **1915**, *37*, 47–70.

(9) Holland, F. A.; Chapman, F. S. *Liquid mixing and processing in stirred tanks*; Reinhold Pub. Corp., 1966.

(10) Kern, D. Q. *Process Heat Transfer, Chapter 18*; Chemical Engineering Series; McGraw-Hill Inc, 1965.

(11) Kays, W. M.; London, A. L. *Compact heat exchangers*, 3rd ed.; McGraw-Hill Inc, 1984.

(12) Runge, C. *Mathematische Annalen* **1895**, *46*, 167–178.

(13) Perry, R.; Green, D. *Perry's Chemical Engineers handbook*, 7th ed.; McGraw-Hill Inc, 1997.

(14) RA-48 Series Reactors Datasheet. Pfaudler Inc., 1998.